# Magnetic Power Loss Estimation in Coaxial Magnetic Gears

M. Filippini [1], P. Alotto[1], E. Bonisoli[2], C. Ragusa[3], M. Repetto[3], A. Vigliani[3]
[1]University of Padova, Department of Industrial Eng., Padova, Italy
[2]Politecnico di Torino, Dept. of Mechanical and Aerospace Eng., Torino, Italy
[3]Politecnico di Torino, Department of Energy Eng., Torino, Italy

## Abstract

This paper proposes a procedure for computing magnetic loss in the iron regions of coaxial magnetic gears. These magnetic structures are made of permanent magnets and ferromagnetic poles in relative motion transferring torque between two shafts in a contactless way. The losses computation in magnetic materials is crucial to define the magnetic transmission performance. Flux distribution inside ferromagnetic parts is computed by means of finite element and cell method and then a model of iron losses taking into account the rotational nature of the flux loci is applied. The procedure will become part of an electro-mechanical model for the evaluation of the whole chain of power conversion both in static and in dynamic conditions.

## FEM Modelling

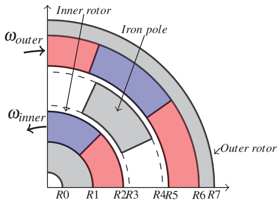


Figure 1: Magnetic gear subdomains.

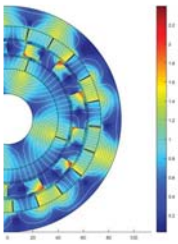

Figure 2: Magnetic flux density $B$ in T and contour of $Az$.

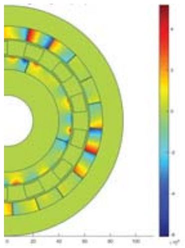

Figure 3: PMs eddy current density $Je$ in $A/m^2$.

The 2D $A$ formulation is adopted, an additional equation for each PM is added to impose the solenoidal property on the eddy currents, $\int_V \mathbf{J_e} dV = 0$.

$$\begin{cases} \nabla \times (\nu \nabla \times \mathbf{A}) = -\sigma \frac{\partial \mathbf{A}}{\partial t} - \sigma \frac{V^i_{PM}}{L} \mathbf{e_z} + \nabla \times (\nu \mathbf{B_r}) \\ \int_V \mathbf{J_e} dV = \int_V (-\sigma \frac{\partial \mathbf{A}}{\partial t} - \sigma \frac{V^i_{PM}}{L} \mathbf{e_z}) dV = 0 \end{cases} \tag{1}$$

where $\sigma$ is the magnet conductivity, $L$ is the machine length, $-\sigma \frac{V^i_{PM}}{L} \mathbf{e_z}$ is the additional current density term and $V^i_{PM}$ is the equivalent voltage drop across the $i^{th}$ PM that ensures the solenoidal property.

## Loss Model

Loss separation: total loss $W$ is expressed as $W = W_{hyst} + W_{exc} + W_{class}$, the sum of the hysteresis, excess, and classical components, and the connection with their unidirectional (scalar) counterpart.

$$W_{hyst}(J_p, a) \simeq W^{(ALT)}_{hyst}(J_p) + W^{(ALT)}_{hyst}(aJ_p)\left(R_{hyst}(J_p) - 1\right) \tag{7}$$

where $R_{hyst} = W^{(ROT)}_{hyst} / W^{(ALT)}_{hyst}$ is the experimental ratio between the hysteresis losses obtained under circular and alternating polarization, $J_p$, expressed as $J_p = B_p - \mu_0 H_p$, is the peak polarization measured along the major axis of the ellipse, and $a$ is the ratio between minor to major axis lengths ($a = 0$, alternating loss; $a = 1$, rotating loss). The excess loss is expressed as:

$$W_{exc}(J_p, a, f) \simeq g(a) \frac{\sqrt{f}}{\sqrt{f_0}} \cdot \left\{ W^{(ALT)}_{exc}(J_p, f_0) + W^{(ALT)}_{exc}(aJ_p, f_0) \left[ \frac{R_{exc}(J_p)}{g(1)} - 1 \right] \right\} \tag{8}$$

where $W^{(ALT)}_{exc}(J_p, f_0)$ is the excess loss obtained under alternating conditions at peak polarization $J_p$ and at the reference frequency $f_0 = 50\,Hz$, $R_{exc}(J_p)$ is the experimental ratio, at a given frequency, between the excess losses obtained under circular and alternating polarization and the function:

$$g(a) = \frac{\sqrt{2\pi}}{8.76} \int_0^{2\pi} \left( \sin^2(\varphi) + a^2 \cos^2(\varphi) \right)^{3/4} d\varphi \tag{9}$$

$g(1) = 1.8$ is the function $g(a)$ calculated for circular polarization ($a = 1$). The classical loss, under negligible skin effect, at frequency $f$ is obtained as:

$$W_{class} = \frac{\sigma d^2}{12} \int_0^{1/f} \left[ \left( \frac{dB_x}{dt} \right)^2 + \left( \frac{dB_y}{dt} \right)^2 \right] dt \tag{10}$$

where $B_x(t)$ and $B_y(t)$ are the induction components.

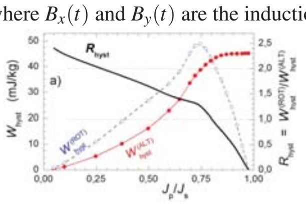


Figure 5: Same material described in [4]: behaviour of the hysteresis alternating and rotational losses versus $J_p/J_s$ at 50 $Hz$ and their ratio.

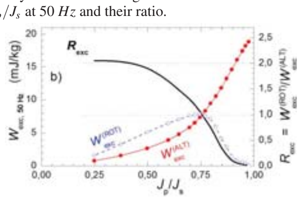


Figure 6: Same material described in [4]: behaviour of the excess alternating and rotational losses versus $J_p/J_s$ at 50 $Hz$ and their ratio.

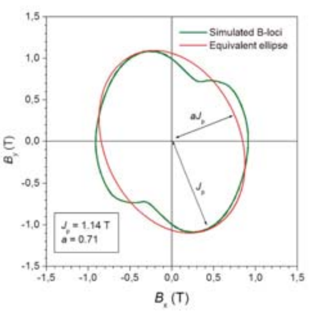


Figure 7: B-locus at a given point within the iron pole: computed cycle and equivalent ellipsoidal one.

## Cell Method Modelling

The approach extensively explained in [2] is adopted. The stiffness matrix A is written as:

$$A = \tilde{C} M_\nu C \tag{2}$$

where C and $\tilde{C}$ are primal and dual curl matrices and $M_\nu$ is the magnetic constitutive matrix built as diagonal considering the sides of the cells as orthogonal. The iron pole material can be either linear or nonlinear, permanent magnets are considered to have $\mu_0$ permeability. The coercive $Hc$ field is projected along dual edges and then assigned as known term:

$$b_{geo} = \tilde{C} F_{Hc} \tag{3}$$

Nonlinearity is treated by Fixed Point by using a constant reluctivity value $\nu_{FP}$ and adding a magneto-motive force term to the RHS. Residual is computed as:

$$R = H - \nu_{FP} |B| \tag{4}$$

Residual is projected along the magnetic flux density direction and then assigned to the RHS as:

$$b_{FP} = \tilde{C} R \tag{5}$$

The solution is then obtained by:

$$A a = b_{geo} + b_{FP} \tag{6}$$

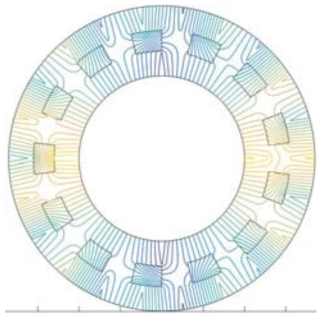

Figure 4: Cell method: magnetic vector potential contour.

## Losses Vs. Speed

The losses varying the rotational speed are computed according to the presented model at the maximum torque capability. PM losses are computed as $\int_V \frac{1}{\sigma'} J_e^2$, where $\sigma' = \frac{\sigma_{PM}}{n_{segm}^{1.65}} = \frac{\sigma_{PM}}{10}$ to consider the PMs segmentation effects.

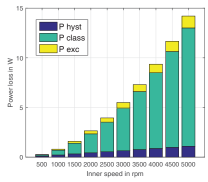


Figure 8: Iron poles losses component for different rotational speeds.

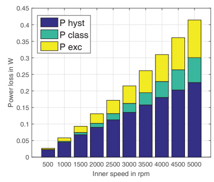


Figure 9: Inner iron yoke component for different rotational speeds.

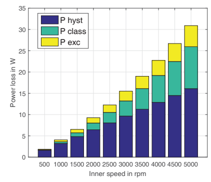


Figure 10: Outer iron yoke component for different rotational speeds.

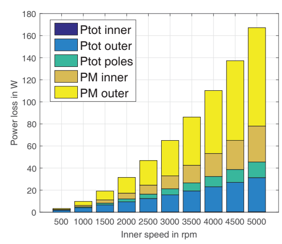


Figure 11: Global losses components for different rotational speeds.

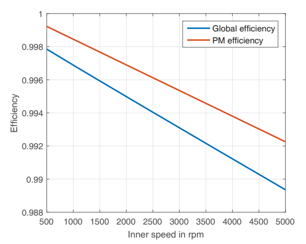


Figure 12: Magnetic gear efficiency at the maximum torque capability.

## Conclusions

Coaxial magnetic gear power losses are analyzed in this paper. An approach for the losses computation with rotational loci is presented and the losses varying the rotational speed are computed for a test case geometry.

## References

[1] K. Atallah, D. Howe, *"A novel high-performance magnetic gear"*, vol. 37. IEEE Transactions on magnetics, 2001, pp. 2844-2846.

[2] P. Alotto, F. Freschi, M. Repetto, C. Rosso, "The Cell Method for Electrical Engineering and Multiphysics Problems, An Introduction", Lecture Notes in Electrical Engineering, Springer-Verlag Berlin Heidelberg, 2013, pag. 141.

[3] C. Ragusa, C. Appino, and F. Fiorillo, "Magnetic losses under two-dimensional flux loci in FeSi laminations", Journal of Magnetism and Magnetic Materials, vol. 316, pp. 454-457, 2007.

[4] C. Appino, M. Khan, O. de la Barriere, C. Ragusa, F. Fiorillo, "Alternating and rotational losses up to magnetic saturation in non-oriented steel sheets", IEEE Transactions on Magnetics, vol. 52, 2016.